

Lawrence Berkeley National Laboratory

LBL Publications

Title

Protection Heater Design Validation for the LARP Magnets Using Thermal Imaging

Permalink

<https://escholarship.org/uc/item/1r9560pw>

Journal

IEEE Transactions on Applied Superconductivity, 26(4)

ISSN

1051-8223

Authors

Marchevsky, M
Turqueti, M
Cheng, DW
et al.

Publication Date

2016-06-01

DOI

10.1109/tasc.2016.2530161

Peer reviewed

Protection Heater Design Validation for the LARP Magnets Using Thermal Imaging

M. Marchevsky, M. Turqueti, D. W. Cheng, H. Felice, G. Sabbi, T. Salmi, A. Stenvall, G. Chlachidze, G. Ambrosio, P. Ferracin, S. Izquierdo Bermudez, J. C. Perez, and E. Todesco

Abstract—Protection heaters are essential elements of a quench protection scheme for high-field accelerator magnets. Various heater designs fabricated by LARP and CERN have been already tested in the LARP high-field quadrupole HQ and presently being built into the coils of the high-field quadrupole MQXF. In order to compare the heat flow characteristics and thermal diffusion timescales of different heater designs, we powered heaters of two different geometries in ambient conditions and imaged the resulting thermal distributions using a high-sensitivity thermal video camera. We observed a peculiar spatial periodicity in the temperature distribution maps potentially linked to the structure of the underlying cable. Two-dimensional numerical simulation of heat diffusion and spatial heat distribution have been conducted, and the results of simulation and experiment have been compared. Imaging revealed hot spots due to a current concentration around high curvature points of heater strip of varying cross sections and visualized thermal effects of various interlayer structural defects. Thermal imaging can become a future quality control tool for the MQXF coil heaters.

Index Terms—Quench protection, superconducting magnets, thermal imaging.

I. INTRODUCTION

QUENCH protection of superconducting accelerator magnets is essential for their reliable operation. The goal of protection is to dissipate magnet stored energy quickly and uniformly upon detecting a quench, thus preventing a possible performance degradation due to formation of a localized hot spot. This goal is accomplished through rapid heat injection into the magnet coil winding that brings it to a normal state. The most common method of heat injection is using “protection heaters”—thin polyimide sheets laminated with stainless steel

Manuscript received October 20, 2015; accepted February 9, 2016. Date of publication March 16, 2016; date of current version March 24, 2016. This work was supported in part by the DOE via the US-LARP program and by the High Luminosity LHC project. The works of A. Stenvall and T. Salmi were supported by the Academy of Finland under Grants 250652 and 287027.

M. Marchevsky, M. Turqueti, D. W. Cheng, H. Felice, G. Sabbi are with the Lawrence Berkeley National Laboratory, Berkeley, CA 94720 USA (e-mail: mmartchevskii@lbl.gov).

T. Salmi was with the Lawrence Berkeley National Laboratory Berkeley, CA 94720 USA. She is now with the Department of Electrical Engineering, Tampere University of Technology, 33720 Tampere, Finland.

A. Stenvall is with the Department of Electrical Engineering, Tampere University of Technology, 33720 Tampere, Finland.

G. Chlachidze and G. Ambrosio are with the Fermi National Accelerator Laboratory, Batavia, IL 60510 USA.

P. Ferracin, S. Izquierdo Bermudez, J. C. Perez, and E. Todesco are with the European Center for Nuclear Physics, 1211 Geneva, Switzerland.

Color versions of one or more of the figures in this paper are available online at <http://ieeexplore.ieee.org>.

Digital Object Identifier 10.1109/TASC.2016.2530161

that are impregnated with the winding and operated by a current pulse [1]. Recently, another promising coil heating technique exploiting ac inter-filament coupling loss of superconducting cables has been developed [2]. A combination of these two techniques was shown to achieve best efficiency and shortest protection delay in a wide range of magnet operational currents [3]. Such combined protection approach is planned for the MQXF high-field Nb₃Sn magnets that are presently being built by the US LARP and CERN collaboration for the high-luminosity upgrade of the inner triplet of the LHC. [4]. Of those magnets, the MQXFB being the longest (7.15 m) magnet of the triplet with a stored energy of 1.2 MJ/m at operational current has the most stringent protection requirement [5]. Protection heaters efficiency thus needs to be optimized for reliable and redundant operation. There has been an effort recently to explore different heater geometries aiming at such optimization [6]. In this paper we focus on the two basic heater geometries that are relevant for MQXF, and have been implemented in the HQ03a LARP quadrupoles. We perform numerical simulations of heat diffusion and heat flux distribution in those geometries, conduct thermal video imaging, and compare the simulation and experiment results. Potential of thermal visualization as a quality control tool for the future MQXF heaters is also discussed.

II. MQXF HEATER OPTIONS

A. Heater Geometry Options

The simplest protection heater geometry is a strip of uniform cross-section covering a certain number of coil turns. Heaters of this type were used in various HQ LARP quadrupole coils [7]. An advantage of the uniform strip heater is that the entire length of the coil winding underneath is being heated up simultaneously, and thus the only factor limiting such heater performance is the thermal diffusion time needed to propagate a sufficient temperature gradient into the cable through the insulation layer. This emphasizes the importance of having uniform and well-controlled properties of the interface, where variations of epoxy layer thickness and occasional delamination of the heater trace from the cable winding may have a significant effect on heater efficiency. While a uniform strip geometry is proven to work well in the HQ magnet series, it cannot be directly adopted for the 7.15 meter long magnet, as the net resistance of such a long heater would be too high for operating it at safe voltage levels. To overcome this problem, two approaches are being considered. In the first one, segments of the heater strip are over-coated periodically with copper to form low resistance

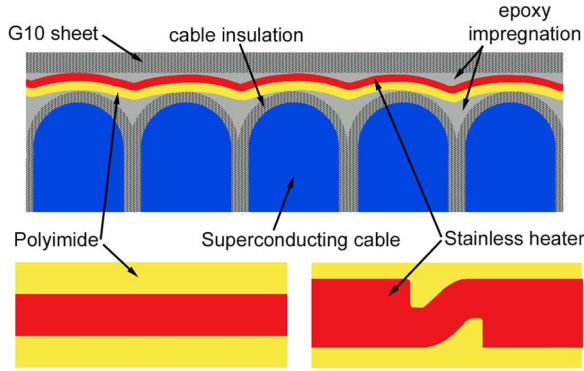


Fig. 1. Top: a cross-sectional view of the heater impregnated with the magnet coil. Bottom: two basic heater geometries used in LARP magnets, a strip of constant cross-section length (left), and a strip of a variable cross-section characterized by a periodic array of narrow width curved "heating stations" placed in-between the wide straight segments (right).

bridges between the so-called heating stations fabricated out of stainless steel. The alternative approach is to periodically change the width of the heater strip along the coil, with wider segments forming the low resistance bridges between heating stations. This approach has been taken in LARP long quadrupole LQ [8], in one of the recent HQ02 hcoil [9], and is also considered as an option for the MQXF. A cross-sectional view of a protection heater trace impregnated with a superconducting coil, and the two basic design patterns discussed are shown in Fig. 1.

B. 2D Simulation of Heat Diffusion

Heat diffusion through insulation materials surrounding the heater can be readily calculated using a numerical method, by solving the heat equation iteratively using finite differences technique. This approach was used successfully to predict heat delays in various LARP magnets [10]. Here we use the same technique to simulate heat diffusion at ambient conditions for a thin heater layer embedded in a composite insulation and placed on top of the superconducting cable. Our model geometry is a multi-layered stack [Fig. 2(a)] that includes a 25- μm -thick stainless steel heater layer on a 50- μm -thick polyimide substrate, separated by a 100 μm layer of epoxy-impregnated cable insulation from two rounded copper blocks of 0.8 mm curvature radius. Stainless and polyimide layers are modeled as slightly undulated following the shape of the underlying cable turns. At the side opposite to the cable, heater layer is facing a 150- μm -thick layer of epoxy-impregnated cloth. For simplicity, heat diffusivities of epoxy, epoxy-impregnated cloth, and epoxy-impregnated cable insulation are considered to be the same. The temperature is fixed at the initial value of 295 K at all boundaries, while the outer face of the stack is separated from the nearest boundary by a 100- μm -thick layer of very low (10^{-12} m^2/s) heat diffusivity emulating a quasi-adiabatic condition at the surface open to the outside air. Radiative heat losses were ignored. Room temperature values of heat conductance and heat capacity for all materials were used. The simulation was performed with a constant time step of 0.1 μs , assuming uniform surface power density and exponential decay of heater current with a time constant of 20.25 ms (taken similar

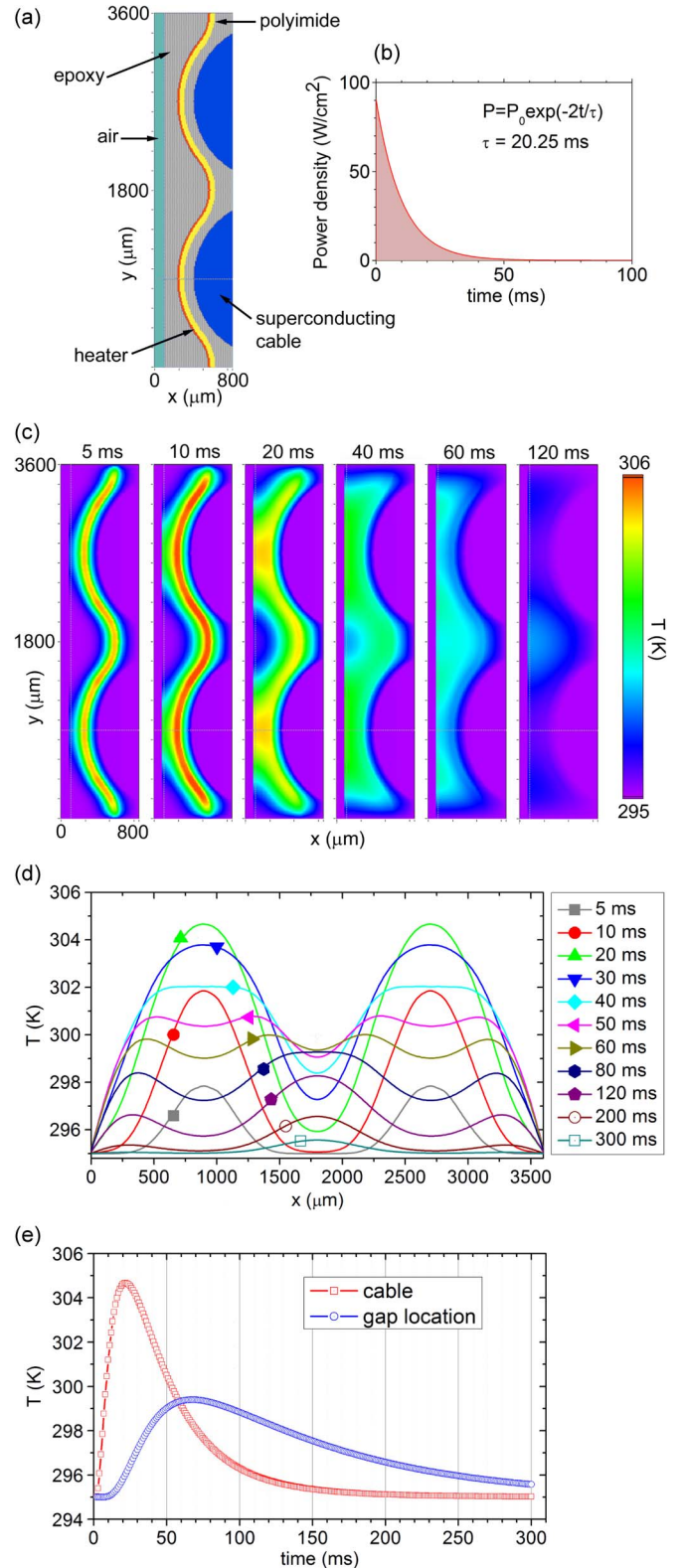


Fig. 2. (a) Heater stack setup used for the 2D heat diffusion simulation. (b) Time dependence of the heater power assumed for the simulation. (c) A sequence of 2D heat maps calculated at various time intervals from the onset of heater firing. (d) Temperature profiles calculated along the outer surface of the heater stack at various time intervals. (e) Time dependences of surface temperature at $y = 900 \mu\text{m}$ (cable location) and $y = 1800 \mu\text{m}$ (gap between the cable turns). Temperature peaks sequentially in those locations with a ~ 50 ms interval. Characteristic thermal relaxation time constants past the peak are ~ 35 ms and ~ 127 ms respectively.

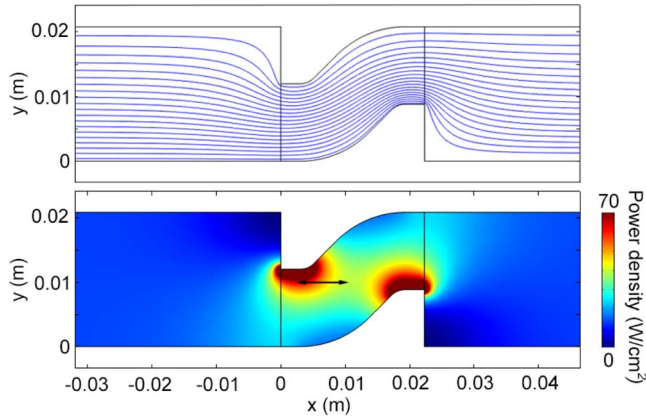


Fig. 3. Result of a simulation for the current flow lines (top) and surface power distribution (bottom) in a single period of a heater strip of variable cross-section. Power deposition peaks locally at the curvature end points. The power density variation the middle of the heating station towards the hot spot along the central line (depicted with an arrow) is $\sim 58\%$.

to the experimental value). Results are shown in Fig. 2(a)–(e). A peculiar evolution of the undulated temperature profile is observed: the surface temperature initially peaks at the locations closest to heater surface, but later on the profile becomes inverted as the peaks transform to the valleys and the new temperature maxima arise at locations in-between the cable turns.

C. Effect of Curvatures to the Heating Power Distribution

An important additional source of inhomogeneous heat deposition in the heater of variable cross-section is a non-uniform current distribution near the curvature points at the heating station ends. This distribution can be readily derived using equipotential lines approach. In Fig. 3 results of current flow and heating power calculation performed in Comsol for a single heating station biased with 10 V is shown. Current flow concentrates near the curvature end points resulting in a formation of localized hot spots. As our heat diffusion simulation assumed a uniform power density across the heater, it would be an important next step to understand how the curvature point hot spots may affect thermal diffusion time and ultimately, the protection performance.

III. THERMAL IMAGING

Thermal imaging is an efficient tool for mapping temperature distribution and identifying thermal inhomogeneity. We used this technique to measure the time-dependent temperature distribution for different heater patterns and compare the measurements to our simulation results. Time-resolved video sampling of thermal images allows to directly evaluate thermal diffusion rate, and detect spatial variation of heat diffusivity. For our experiments we used a Keysight U5855A TrueIR Thermal Imager camera with 0.1 K sensitivity interfaced to a PC-based frame grabber software. The camera was installed on a tripod above the magnet coil, facing the heater strip. The heater was powered with a unit containing a capacitor that was initially charged to 150–350 V and then discharged into the heater strip using a manually-triggered SCR circuit, resulting in characteristic power densities of $\sim 50\text{--}200\text{ W/cm}^2$ in the

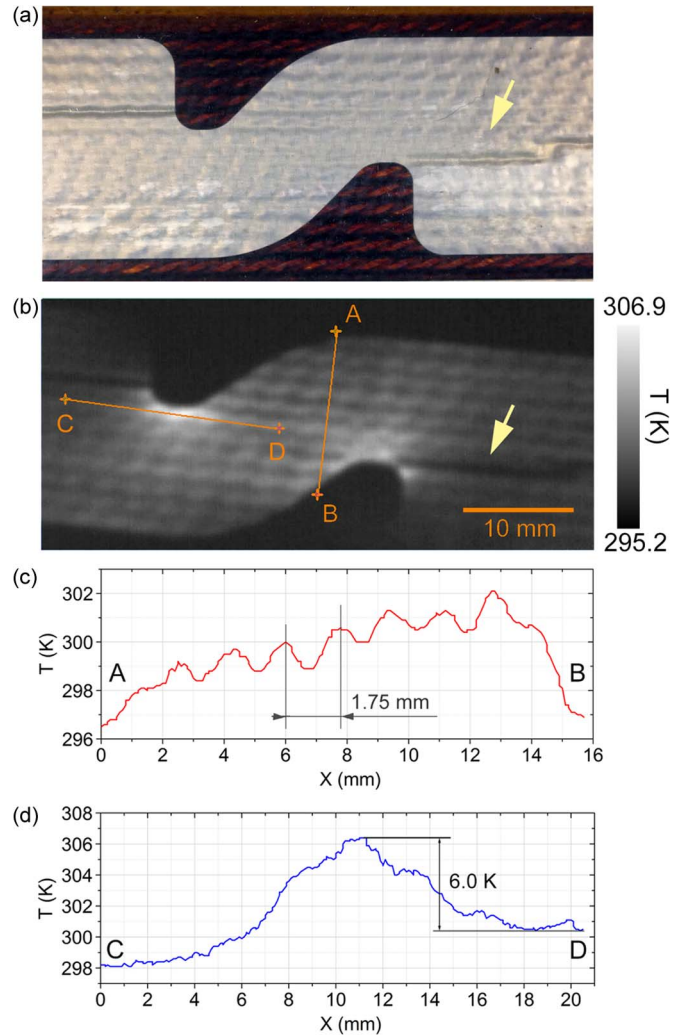


Fig. 4. (a) A photograph of the heating station at the coil outer surface. (b) The first thermal image taken past the current spike in the heater. (c) Temperature distribution in the direction perpendicular to the turns. A periodic distribution pattern resembling the underlying cable structure is seen. (d) Temperature distribution along the median line showing temperature rise towards a hotspot.

heater. IR images were acquired continuously throughout the heater firing and the following thermal relaxation process by the camera at 9 frames/s internal rate and the video stream was up-sampled to 25 frames/s by a PC software.

A. Imaging of the QXF-Style Heater of Variable Cross-Section

We performed time-resolved thermal imaging on the outer layer heater of variable cross-section with periodic heating stations. This heater was installed on the HQ Coil 26 of HQ03a LARP quadrupole; a spare coil with identical design was used for imaging studies. Heaters were formed with photolithography in 25 μm thick stainless steel, and laminated over 50 μm thick polyimide film. The heater was impregnated to the coil wound with 1.6 mm thick Nb_3Sn Rutherford cable on top of the heater is $\sim 150\ \mu\text{m}$ thick. Each heating station is 12 mm wide and spans at 45 deg. angle in-between the 20.8 mm wide straight strip sections. A photograph of the heating station is shown in Fig. 4(a). An undulated surface profile of the stainless layer following the underlying cable structure is

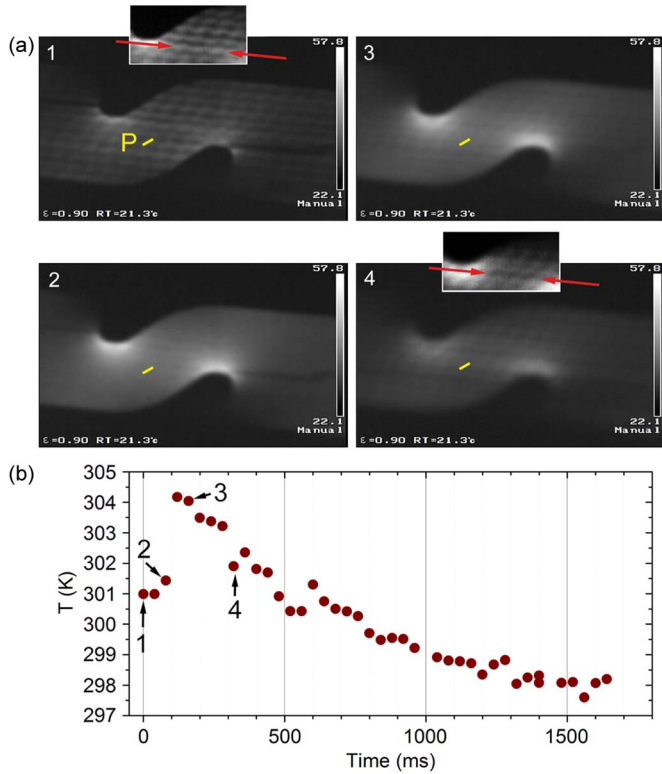


Fig. 5. (a) Thermal images (direct camera views) taken sequentially past the heater powering with time intervals of t_{12} and t_{23} of 80 ms and t_{34} of 160 ms. A zoomed-in region near the hot-spot showing details of the modulated pattern is shown in the insets of Images 1 and 4. (b) Temporal evolution of the temperature calculated by averaging values along a 10 pixel line (marked “P”) in the middle of the heating station. The data points corresponding to the images shown in (a) are labeled.

clearly visible through the optically-transparent top layer of epoxy-impregnated insulation. One should note, however, that insulation transparency in the wavelength interval of 8–14 μm relevant for thermal imaging is quite small, and therefore only the exposed top surface of the insulation layer is being imaged in our experiments. The heater was pulsed using a capacitor bank of 0.56 mF charged to 300 V, yielding a 85 A spike of heater current followed by decay with time constant of 20.25 ms. Imaging result is shown in Fig. 4(b). One can clearly distinguish a periodic thermal modulation caused by the varying distance between the heater and the top insulation insulated with 100 μm thick layer of S-glass. The insulation layer. The measured temperature distribution period of 1.75 mm, as seen from the A-B cross-sectional plot [Fig. 4(c)], matches the expected inter-turn separation of ~ 1.8 mm. Two hot spots are observed around the curved end points of the heating station. The temperature rise from the center of the heating station towards the hot spot measured along the median C-D line is ~ 6.0 K [Fig. 4(d)], or when normalized to $T_D - T_A$, it is 50%—in good agreement with the simulation result. An impregnation defect causing the heater layer to wrinkle and slide deeper into the groove between neighboring turns is also clearly revealed in the thermal image [shown with arrows in Fig. 4(a) and (b)]. Its dark appearance is consistent with a thicker layer of impregnation epoxy separating heater from the top surface. Images of the temporal evolution of the surface

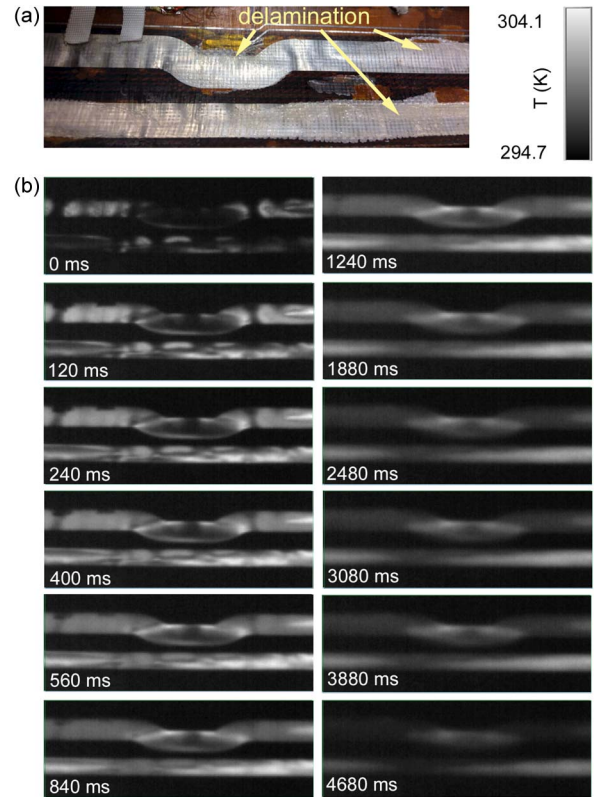


Fig. 6. (a) A photograph of the HQ Coil 20 inner layer heater exhibiting delamination defects (marked with arrows) after two magnet cold tests. (b) A sequence of thermal images showing strong inhomogeneity of thermal distribution due to delamination defects, and its temporal evolution. Labels show elapsed time intervals relative to the first acquired image.

temperature are shown in Fig. 5. As heater power is decreasing to zero, a more uniform distribution without a pronounced short-scale modulation emerges (Image 2). Later on, as heat is being transferred into the cable, a modulated pattern re-emerges again (Image 4), but now it is inverted with respect to the initial one, as shown in the insets of Images 1 and 4. This is in qualitative agreement with our heat diffusion simulation results. A thermal relaxation time constant extracted from the data in Fig. 5(b) is ~ 685 ms. This is substantially longer than that obtained in the simulation, thus suggesting a poorer thermal interface contact between the heater and its neighboring layers, a thicker than expected layer of insulation (including the epoxy) built into the heater stack during impregnation, or a combination of these factors. A more involved modelling of thermal properties of the insulation and the underlying cable geometry may be required to account for the quantitative discrepancy between the calculated and measured time constant.

B. Imaging of the HQ-Style Heater of Constant Cross-Section.

An HQ-style strip heater of constant width installed at the inner layer of HQ02 coil has been imaged after that coil removal from HQ02 magnet following two magnet cold tests. As the heater strips were fired over hundred times during magnet training and quench heater studies, they developed numerous local delamination defects. An example is shown in the photograph of Fig. 6(a). Upon firing this heater (at the capacitor voltage

350 V and the time constant of ~ 40 ms), thermal imaging revealed such defects clearly [Fig. 6(b)]. For example, the central portion of the U-shaped heater part exhibits a heavily delaminated area; in thermal images it initially stays dark for up to ~ 600 ms thus suggesting a delamination between the heater and top layer of insulation. But after ~ 3000 ms pass, most of the heater strip cools down while the area of interest stays warm and eventually turns bright in the image. It is therefore plausible to assume that the thermal contact between the heater layer and the coil is also poor in that area, hinting at a delamination been present at both sides of the heater. While it is hard to distinguish by visual inspection which side of the heater is delaminated, thermal imaging provides an alternative non-destructive way of performing this determination.

IV. CONCLUSION

Thermal imaging is a direct and sensitive technique to characterize heat diffusion in the impregnated heaters of high-field accelerator magnets. Timed acquisition of thermal images allows probing of the local thermal diffusion characteristics of the heater stacks, and facilitates non-destructive qualification of delamination defects. Thermal imaging appears to be a promising and useful technique for quality assurance evaluation of future QXF coils during production, as well as nondestructive evaluation of heater defects caused by their operation in magnet cold tests.

ACKNOWLEDGMENT

Authors are thankful to J. Swanson and T. Lipton for assistance in coil preparation.

REFERENCES

- [1] H. Felice *et al.*, "Instrumentation and quench protection for LARP Nb₃Sn magnets," *IEEE Trans. Appl. Supercond.*, vol. 19, no. 3, pp. 2458–2462, Jun. 2009.
- [2] E. Ravaoli *et al.*, "New, coupling loss induced, quench protection system for superconducting accelerator magnets," *IEEE Trans. Appl. Supercond.*, vol. 24, no. 3, Jun. 2014, Art. ID 0500905.
- [3] E. Ravaoli *et al.*, "Protecting a full-scale Nb₃Sn magnet with CLIQ, the new coupling-loss-induced quench system for high-luminosity upgrade of the inner triplet of the LHC.," *IEEE Trans. Appl. Supercond.*, vol. 25, no. 3, Jun. 2015, Art. ID 4001305.
- [4] G. Ambrosio, "Nb₃Sn high field magnets for the high luminosity LHC upgrade project," *IEEE Trans. Appl. Supercond.*, vol. 25, no. 3, Jun. 2015, Art. ID 4002107.
- [5] E. Todesco, "Quench limits in the next generation of magnets," in *Proc. WAMSDO Workshop*, 2013, pp. 10–16.
- [6] T. Salmi *et al.*, "Protection heater delay time optimization for High-Field Nb₃Sn accelerator magnets," *IEEE Trans. Appl. Supercond.*, vol. 24, no. 3, Jun. 2014, Art. ID 4701305.
- [7] H. Felice *et al.*, "Design of HQ—A high field large bore Nb₃Sn quadrupole magnet for LARP," *IEEE Trans. Appl. Supercond.*, vol. 19, no. 3, pp. 1235–1239, Jun. 2009.
- [8] G. Ambrosio *et al.*, "LARP long Nb₃Sn quadrupole design," *IEEE Trans. Appl. Supercond.*, vol. 18, no. 2, pp. 268–272, Jun. 2008.
- [9] J. DiMarco *et al.*, "Test Results of the LARP HQ03a Nb₃Sn Quadrupole," *IEEE Trans. Appl. Supercond.*, to be published.
- [10] T. Salmi *et al.*, "A novel computer code for modeling quench protection heaters in high-field Nb₃Sn accelerator magnets," *IEEE Trans. Appl. Supercond.*, vol. 24, no. 5, Aug. 2014, Art. ID 4701810.